

Original Research

# Vegetation Cover and Its Relationships with Topography and Climate in Cameroon (2000-2022)

Chuanxin Liu, Yong Du<sup>✉\*</sup>, Chunhua Shi

Jiyang College of Zhejiang A&F University, Zhejiang, China

Received: 22 August 2025

Accepted: 15 March 2026

## Abstract

Climate change and human activities have significantly altered ecosystems worldwide, leading to changes in vegetation cover, especially in tropical and arid regions. In Central Africa, Cameroon is experiencing rapid shifts in vegetation patterns due to both climatic factors and land-use practices. Understanding these spatiotemporal changes is crucial for developing effective strategies for ecological protection and restoration. This study examines the spatiotemporal dynamics of vegetation cover in Cameroon from 2000 to 2022 and explores their relationships with topographic and climatic drivers. Utilizing remote sensing and GIS, we integrated MODIS imagery, meteorological station records, and digital elevation models to analyze fractional vegetation cover (FVC) patterns across Cameroon's regions. Our results reveal marked spatiotemporal variations in FVC over the past 23 years: southern tropical rainforests are increasingly threatened by climate change and human activities, while northern savannas face an increasing risk of desertification. In arid and semi-arid zones, vegetation growth is closely linked to precipitation and temperature. Furthermore, topographic variables such as elevation and slope strongly modulate vegetation distribution and growth. These findings illustrate the complex interplay between climatic and physiographic drivers governing vegetation dynamics in Cameroon and provide a scientific basis for targeted ecological protection and restoration strategies.

**Keywords:** vegetation coverage, physiography, climate, remote sensing, ecological security, spatiotemporal evolution

## Introduction

The Sixth Assessment Report (AR6) by the Intergovernmental Panel on Climate Change (IPCC) has revealed a stark reality: from 2011 to 2020, global surface temperatures rose by 1.09°C relative to pre-

industrial levels, with a projected probability exceeding 90% that global temperature will surpass 1.5°C by 2035 [1]. This temperature rise has profound implications for ecosystems, particularly regarding land surface temperature (LST) and its interaction with fractional vegetation cover (FVC) [2, 3]. The relationship between LST and FVC is critical as vegetation plays an integral role in the terrestrial carbon cycle, influencing climate feedback mechanisms. Understanding the dynamic responses of FVC over time and space has therefore become a central focus in climate change and ecological studies [4].

\*e-mail: duyongstu@163.com

Tel.: +86 18966162106

0000-0001-8164-8500

While substantial progress has been made in understanding FVC dynamics, a critical regional knowledge gap persists: most existing studies focus on temperate and high-latitude ecosystems (e.g., the Loess Plateau [5], Hulunbuir Grassland [6], Huaihe River Basin [7]), with limited systematic analyses of tropical regions, particularly Central Africa. Tropical zones, characterized by complex topography, high biodiversity, and vulnerability to climate extremes, play a disproportionate role in the global carbon cycling and climate regulation [8]. Yet, their FVC responses to environmental drivers remain poorly quantified. This gap is especially pronounced for Cameroon, a microcosm of African climate dynamics due to its diverse topography (from coastal plains to mountainous regions) and bimodal rainfall regime. Despite its ecological significance, Cameroon's spatiotemporal FVC patterns and driving mechanisms have not been comprehensively investigated using long-term remote sensing data, a void this study aims to fill.

Existing studies in non-tropical regions highlight key drivers of FVC, particularly in relation to topography and climate. For instance, shaded slopes had 12.7% higher FVC than sunny slopes, with FVC increasing by 2.1% for every 100-meter increase in elevation on the Loess Plateau [5]. Studies in regions like Hulunbuir Grassland have found that long-term grazing activities on steeper slopes reduced FVC's sensitivity to precipitation by 34% [6]. Similarly, in the Huaihe River Basin, a 1°C temperature increase in areas above 500 meters led to a 0.9% reduction in FVC, a stark contrast to the 0.3% decrease observed in flatlands [7]. These studies demonstrate the significant role that terrain plays in shaping vegetation dynamics, with scholars such as Woodcock and Strahler laying the groundwork for subsequent analyses on terrain effects on vegetation remote sensing [9]. Other studies, including those by Lan et al., have quantitatively analyzed the terrain-FVC relationships, particularly in the Qinghai-Tibet Plateau [10], while Lai and Shi focused on the coupling dynamics of climate, human activity, and terrain in southwest China's high-mountain regions [11]. Du et al.'s research further confirmed that topography could explain 35-48% of FVC variability in temperate zones [12]. Additionally, advancements in remote sensing technologies, such as microwave vegetation optical depth (VOD), have enhanced the accuracy of FVC estimates, surpassing traditional indices like the normalized difference vegetation index (NDVI) in estimating gross primary productivity (GPP) [13]. Recent advancements, such as projections of land-cover change in tropical high-Andean lakes [14], soil erosion risk mitigation in steep forest ecosystems [15], and mangrove mapping using Sentinel-2 imagery [16], underscore the need for integrating anthropogenic factors like deforestation and agricultural expansion into FVC analyses, which are often overlooked in Central African studies.

This study improves upon previous regional assessments by employing a multi-method approach

(e.g., combining parametric Slope regression with non-parametric Theil-Sen and Mann-Kendall tests) on long-term (23-year) MODIS data at the national scale, explicitly incorporating anthropogenic drivers inferred from land-use maps and population data, and quantifying their relative contributions to FVC changes, addressing limitations in prior studies that often relied on shorter time series or ignored human influences. This study aims to fill this gap by comprehensively analyzing the spatiotemporal dynamics of FVC in Cameroon over 23 years (2000-2022), utilizing MODIS Enhanced Vegetation Index (EVI), the Shuttle Radar Topography Mission (SRTM) Digital Elevation Model (DEM), and CRU TS 4.06 climate data [17]. A combination of the Slope, Sen, and Mann-Kendall methods and ArcGIS spatial analysis will be applied to explore how topographic factors, such as elevation and slope, regulate FVC. Additionally, the study will use a multiple regression model to assess the influence of climate factors such as precipitation, surface temperature, and solar radiation on FVC. The long-term trends and stability of FVC will be analyzed using the Hurst exponent, providing insights into vegetation resilience in the face of climate change. Cameroon's geographical and climatic diversity offers a unique case for studying FVC, with implications for both local climate adaptation and global ecological models. This research contributes to the scientific foundation of China-Africa cooperation initiatives, particularly in the context of green development projects under the Belt and Road Initiative. It also holds practical value for policy formulation in climate adaptation and offers a remote sensing framework for monitoring initiatives like the African Great Green Wall [18-22]. By addressing these critical gaps, this study will enhance our understanding of vegetation dynamics in tropical regions and improve global climate and ecological models.

## Materials and Methods

### Study Region

Cameroon (Fig. 1), located in west-central Africa (2°13'-13°05' N, 8°22'-16°11'30" E), spans an area of 475,600 km<sup>2</sup> and is shaped like an inverted triangle that widens in the south and narrows in the north. It borders the Chad-Nigerian Sahel region to the north, faces the Gulf of Guinea to the south, adjoins the Central African-Congolese rainforest to the east, and connects to the Nigerian Highlands to the west, sharing a 5,213 km border with six neighboring countries. The country's diverse topography and latitudinal gradients give rise to three major climatic zones (Table 1): the Southern Equatorial Rainforest Zone, with an annual average temperature of 25-28°C and annual precipitation ranging from 2,000 to 4,000 mm, representing a typical equatorial climate; the Central Tropical Savanna Zone, with an annual average temperature of 24-30°C

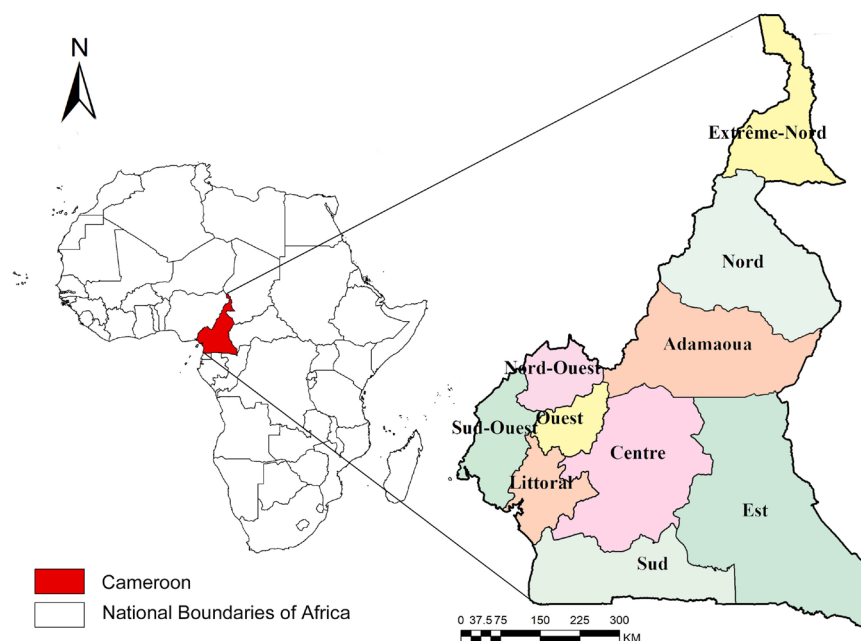


Fig. 1. Regional map of Cameroon.

Table 1. Grading of the vegetation coverage.

Grading Standards	Vegetation Cover Degree (FVC)	Nationwide	Far North and Northern Regions	Mountainous Regions	Centre, South, and East Regions
Low Coverage	0-20	2.73%	10.72%	1.02%	0.13%
Moderately Low Coverage	20-40	8.01%	33.42%	1.75%	0.22%
Moderate Coverage	40-60	19.42%	46.66%	25.06%	3.45%
Moderately High Coverage	60-80	40.13%	8.87%	56.41%	44.42%
High Coverage	80-100	29.71%	0.33%	15.77%	51.78%

and annual precipitation between 1,500 and 2,000 mm, characterized by distinct wet and dry seasons; and the Northern Sahelian Semi-Arid Zone, with an annual average temperature of 30-34°C and annual precipitation ranging from 500 to 1,000 mm, classified as an extremely arid Sahelian climate [23, 24]. The topography of Cameroon displays a distinct north-south gradient. The southern region is characterized by coastal plains with elevations below 500 m, while the central region is dominated by the 1,000-2,000 m Adamawa Plateau. To the north, the Chad Basin descends to below 300 m, and the western volcanic slopes feature steep gradients exceeding 45°. This diverse topography creates an “Equatorial-Sahelian” hydrothermal gradient and contributes to the region's complex microtopographic heterogeneity. Influenced by a monsoonal climate, the northern Sahelian zone is particularly vulnerable to severe droughts, while the southern coastal areas face frequent heavy rainfall and flooding [25]. These climatic and topographic dynamics underscore the vulnerability of the region's ecosystems.

Cameroon's economy is primarily driven by the primary sector. Agriculture contributes 17% to the country's GDP and accounts for 62.9% of employment. Forest cover spans 46% of the country, supporting an annual growth rate of 4.8% in the forestry sector. Livestock farming employs 30% of the workforce, while annual fish production reaches 233,000 tonnes. Tourism, supported by 45 protected areas and 1.02 million international visitors, plays a significant role in the service sector. In 2022, with a GDP of 44.3 billion USD, oil represented 50% of the country's exports, highlighting the economy's heavy reliance on primary industries, particularly agricultural products [26].

#### Data

This study utilized five datasets from the Google Earth Engine (GEE) platform (<https://earthengine.google.com/>): SRTM 30 m DEM (2000), which was processed in ArcGIS to generate elevation, slope, and aspect layers for Cameroon; MOD13Q1 EVI 250 m monthly product

(2000-2022), selected for its high temporal resolution and suitability for vegetation monitoring in dense canopy areas, selected for its high temporal resolution and suitability for vegetation monitoring in dense canopy areas, with a maximum value composite applied for cloud removal and optimized for densely vegetated areas, and additional quality-assurance filtering to address cloud contamination prevalent in the southern tropical rainforest zones; MOD11A2 LST 1 km daily data (2000-2022) for heat stress analysis; CRU TS 4.05 precipitation data (0.5° resolution, 2000-2022); and solar radiation data from the same source. All datasets were processed in ArcGIS using a unified projection (WGS84/UTM 32N) to create a multiscale dataset encompassing topographic data (30 m), vegetation data (250 m), and climate data (0.5°). To align with the resolution of EVI data, climate and terrain datasets were resampled to a 250 m resolution when investigating the driving mechanisms of FVC spatial patterns. This approach ensures consistency across datasets and enhances the accuracy of spatial analyses.

To address potential biases from multi-resolution integration, such as resolution mismatches (e.g., 250 m EVI vs. 0.5° CRU), cloud contamination in MODIS data, and resampling effects (e.g., bilinear interpolation introducing smoothing artifacts), we implemented quality controls: MODIS data were filtered for low cloud cover (<10%) using quality-assurance flags, and resampling was validated against ground-truth points from meteorological stations to minimize scale-induced uncertainties, which could otherwise underestimate local heterogeneity by up to 15% in correlation analyses [27].

## Methodology

This study follows a three-step approach – trend analysis, correlation analysis, and predictive analysis – using methods implemented on the GEE, ArcGIS, and MATLAB platforms. The analysis incorporates multi-scale (pixel-to-regional) and multi-method (statistical and modeling) cross-validation techniques to explore the coupling mechanisms between topography (elevation/slope), climate (precipitation/LST), and vegetation (EVI) along Cameroon's “Equatorial-Sahelian” gradient.

### 1) FVC estimation

Using the MOD13Q1 EVI (250 m) dataset, the pixel dichotomy method (ENVI 5.2) was applied [28, 29]. FVC was modeled from EVI values rather than direct products, using the dimidiate pixel model to partition pixels into vegetated and non-vegetated components based on pure pixel thresholds [27]. The 0.5%/99.5% percentiles were chosen to exclude extreme outliers (e.g., noise from atmospheric effects), ensuring pure vegetated ( $EVI_{veg}$ ) and soil ( $EVI_{soil}$ ) endmembers while balancing data utilization and model accuracy; sensitivity tests showed that varying thresholds within 2-10% altered FVC by <5%, confirming the robustness of the results.

The estimation followed the model constructed as outlined below:

$$FVC = \frac{EVI - EVI_{soil}}{EVI_{veg} - EVI_{soil}} \quad (1)$$

### 2) Stability assessment

The coefficient of variation (CV) of pixel-scale FVC for 2000 to 2022 was calculated. As an effective measure of data dispersion, CV is particularly suitable for long-term time-series datasets and can reflect the variability of pixel values. Lower CV values indicate higher stability, while higher values suggest greater fluctuations [30].

$$\begin{cases} C_v = \frac{\sigma}{\overline{FVC}} \\ \sigma = \sqrt{\frac{1}{n} \sum_{i=1}^n (FVC_i - \overline{FVC})^2} \end{cases} \quad (2)$$

In the equation,  $C_v$  represents the coefficient of variation of Fractional Vegetation Cover (FVC);

$FVC_i$  denotes the FVC value in the  $i$ -th year; and  $\overline{FVC}$  represents the mean value of FVC.

This study used a combination of analytical methods to enhance robustness: linear regression (Slope) for parametric trend fitting, Theil-Sen median slope for non-parametric noise-resistant trend estimation, and the Mann-Kendall test for significance ( $\alpha = 0.05$ ), classifying trends into grades [31]. This multi-method approach addresses methodological novelty by integrating parametric and non-parametric techniques, improving accuracy in noisy long-term data compared to single-method studies. The EVI slope was calculated using simple linear regression and the least squares method on a pixel-by-pixel basis. This approach quantified long-term EVI trends and assessed both the direction and rate of vegetation cover changes in the study area over multiple years.

$$\text{Slope} = \frac{n \sum_{i=1}^n (i \times EVI_i) - \sum_{i=1}^n i \times \sum_{i=1}^n EVI_i}{n \sum_{i=1}^n i^2 - (\sum_{i=1}^n i)^2} \quad (3)$$

The Theil-Sen median trend analysis calculates the median of slopes from all data pairs in a time series to detect trends. This method is robust to noise and is particularly effective for non-normally distributed data.

$$\theta_z = \text{Median} \left( \frac{X_j - X_i}{j - i} \right), \quad \forall j > i \quad (4)$$

The Sen trend analysis method does not assess the significance of trends. Therefore, the Mann-Kendall test is integrated to effectively validate the significance of the observed trend sequences.

$$S = \sum_{i=1}^{n-1} \sum_{j=i+1}^n \text{sgn}(x_j - x_i) \quad (5)$$

$$\text{sgn}(x_j - x_i) = \begin{cases} 1 & x_j - x_i > 0 \\ 0 & x_j - x_i = 0 \\ -1 & x_j - x_i < 0 \end{cases} \quad (6)$$

$$Z = \begin{cases} \frac{S-1}{\sqrt{\text{VAR}(S)}}, S > 0 \\ 0, S = 0 \\ \frac{S-1}{\sqrt{\text{VAR}(S)}}, S < 0 \end{cases} \quad (7)$$

$$\text{VAR}(S) = \frac{[n(n-1)(2n+5) - \sum_{i=1}^n t_i(t_i-1)(2t_i+5)]}{18} \quad (8)$$

### 3) Driving correlation

Additionally, anthropogenic drivers were quantified using ESA CCI land-use maps to derive deforestation and cropland expansion metrics, integrated into the multiple regression model. The Pearson correlation coefficient is a statistical measure that quantifies the strength of the linear relationship between two variables, with values ranging from [-1, 1]. A larger absolute value indicates a stronger correlation, while the sign indicates the direction of the relationship [32]. The equation is as follows:

$$R_{xy} = \frac{\sum_{i=1}^n [(x_i - \bar{x})(y_i - \bar{y})]}{\sqrt{\sum_{i=1}^n (x_i - \bar{x})^2 \sum_{i=1}^n (y_i - \bar{y})^2}} \quad (9)$$

Using MATLAB, regression models were developed for variables in Cameroon to enable in-depth analysis. The correlation coefficient  $R_{xy}$  represents the strength of the relationship between two variables, where  $\bar{x}$  and  $\bar{y}$  denote the mean values of the respective variables, and  $n$  represents the sample size.

### 4) Persistence prediction

Hurst analysis (i.e., the Hurst exponent) is a key statistical tool used to evaluate long-term dependence and self-similarity in time-series data. In vegetation recovery potential research, this method analyzes long-term trends and the stability of vegetation cover changes, reveals recovery potential and pathways using historical vegetation data, and provides a scientific basis for ecological restoration planning, vegetation dynamics monitoring, and the assessment of human impacts on ecosystems.

$$\overline{\text{FVC}}_{(\tau)} = \frac{1}{\tau} \sum_{t=1}^{\tau} \text{FVC}_{(t)} \quad \tau=1, 2, \dots, n \quad (10)$$

$$X(t, \tau) = \sum_{u=1}^t \text{FVC}_{(u)} - \overline{\text{FVC}}_{(\tau)} \quad 1 \leq t \leq \tau \quad (11)$$

$$R_{(\tau)} = \max_{1 \leq t \leq \tau} X(t, \tau) - \min_{1 \leq t \leq \tau} X(t, \tau) \quad \tau=1, 2, \dots, n \quad (12)$$

$$S_{(\tau)} = \left[ \frac{1}{\tau} \sum_{t=1}^{\tau} (\text{FVC}_{(t)} - \overline{\text{FVC}}_{(\tau)})^2 \right]^{\frac{1}{2}} \quad \tau=1, 2, \dots, n \quad (13)$$

$$\frac{R_{(\tau)}}{S_{(\tau)}} = (c\tau)^H \quad 1 \leq t \leq \tau \quad (14)$$

In the equation,  $H$  represents the Hurst exponent, and  $\tau$  denotes the temporal length of FVC/LAI. The Hurst exponent (0-1) quantifies the persistence of the 23-year FVC trend, where  $H > 0.6$  denotes strong persistence, and  $H < 0.4$  indicates strong antipersistence [33].

To incorporate anthropogenic factors, we inferred human activities from ESA CCI land-use maps (300 m resolution, 2000-2022) and WorldPop population density data (100 m), quantifying drivers like deforestation (e.g., forest-to-cropland conversion rates) and agricultural expansion (e.g., cropland area increase by 15% in northern regions), and these were integrated into multiple regression models to compare with climatic drivers [34].

## Results and Discussion

### FVC Spatiotemporal Variations

#### Distribution Characteristics and Regional Disparities

Cameroon's Fractional Vegetation Cover (FVC) displays pronounced regional disparities driven by a synergy of latitudinal hydrothermal gradients and intensifying human pressures (Table 1, Fig. 2). The southern regions, encompassing the Centre, South, and East provinces, maintain consistently high FVC levels (>51.78% high-coverage area). This is attributed to the bimodal rainfall regime and minimal land disturbance, where deforestation rates remain relatively low (<5%) compared to the North. Conversely, the northern Sahelian regions exhibit significantly lower FVC (10.72% low-coverage area), reflecting both climatic aridity and extensive agricultural expansion, with cropland increasing from 20% to 35% of land cover over the study period [34]. In these fragile zones, desertification risks have increased by 12% [35], as evidenced by localized vegetation declines in protected areas like the Bontioili Reserve.

#### Trend Analysis

Fig. 3 illustrates the spatiotemporal trends in FVC across Cameroon from 2000 to 2022. The data reveal that northern regions, including the Far North, showed a slight increase in FVC ( $R^2 = 0.0325$ , rate = +0.005/year), though weak and indicative of gradual changes.

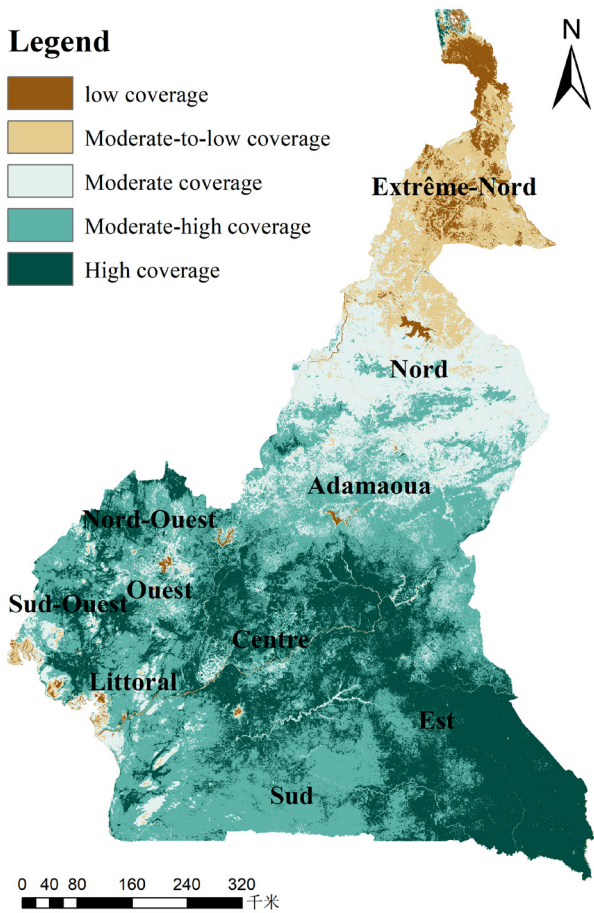


Fig. 2. Mean FVC distribution.

Mountainous regions maintained stable FVC around 60% ( $R^2 = 0.00354$ ), reflecting ecological balance despite fluctuations. Nationwide, FVC averaged approximately 60%, with no significant overall trend. However, central, southern, and eastern regions exhibited a weak upward trend ( $R^2 = 0.0183$ , rate =  $+0.008/\text{year}$ ), suggesting gradual improvement possibly due to reforestation in

protected areas (e.g., Bontoli Reserve) and increased rainfall offsetting localized deforestation reports. Southern tropical rainforests are increasingly threatened by climate change and human activities, consistent with the complex interplay of drivers quantified in this study. Fig. 4 further elucidates the regional distribution: nationwide, medium coverage accounts for 19.42%, medium-high for 40.13%, and high for 29.71%, with low and medium-low comprising the remainder.

Seasonal FVC patterns align with phenological cycles of dominant vegetation types: southern rainforests maintain high FVC year-round due to evergreen broadleaf phenology, while northern savannas peak during wet seasons (June-September) with grass growth cycles. These patterns link explicitly to agricultural cycles, with northern declines in dry seasons (October-May) coinciding with post-harvest grazing and fuelwood collection, reducing FVC by up to 20%. Fig. S2 shows monthly mean FVC, highlighting north-south contrasts; Fig. S3 (monthly stacked chart) illustrates coverage grading variations; regional specifics include Fig. S4 (mountainous stacked), Fig. S5 (central-southern monthly stacked, showing stable high coverage), and Fig. S6 (northern monthly stacked, revealing pronounced seasonal dips).

### Stability Analysis

Fig. 5 shows the interannual stability of FVC: nationwide moderate fluctuations at 55.36%, indicating balanced variability; northern regions exhibit higher fluctuations (20.44%), driven by climatic aridity and human pressures [36]; central-southern areas show lower volatility (9.21%), benefiting from stable conditions (Table 2 for details). Monthly stability (Fig. S7) further confirms these patterns, with greater variability in northern dry months.

Fig. 6 presents trend analyses: Slope & Sen indicate degradation in 25% of northern pixels (rate =  $-0.015/\text{year}$ ), with Mann-Kendall confirming significance

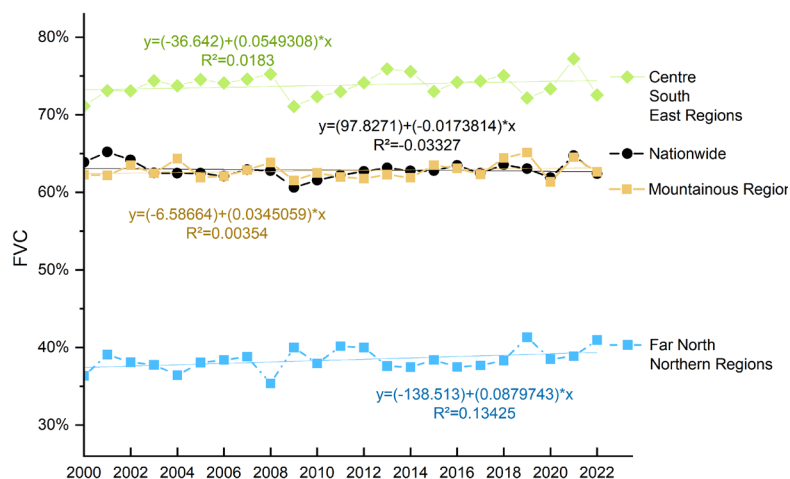


Fig. 3. Annual changes in mean FVC.

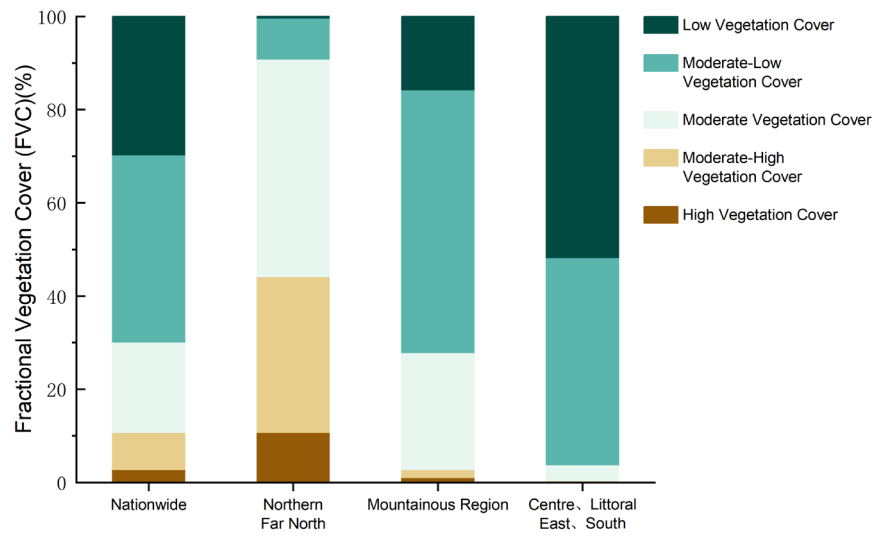


Fig. 4. FVC stacked chart.

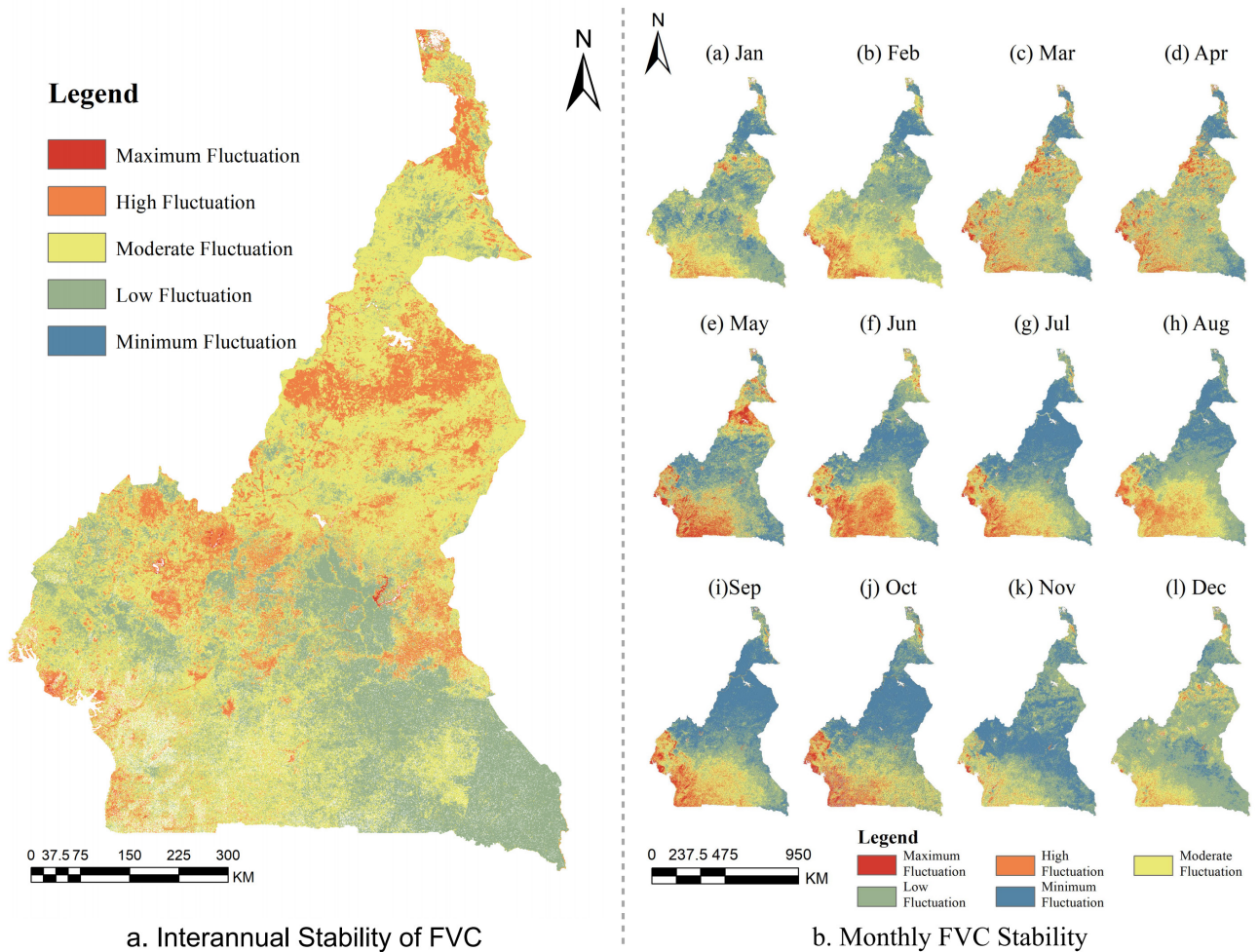


Fig. 5. Spatiotemporal stability analysis of fractional vegetation cover (FVC) in Cameroon (2000-2022). a) Interannual stability and b) monthly stability.

Table 2. Stability of vegetation coverage change in Cameroon from 2000 to 2022.

Climatic Factor	Nationwide	Northern Province, Far North Province	Mountainous Region	Centre Province, Littoral Province, East Province, South Province
Minimum fluctuation	0.00%	0.00%	0.00%	0.00%
Low volatility	27.92%	21.59%	15.50%	46.61%
Moderate fluctuations	55.36%	57.85%	65.86%	44.07%
Higher fluctuations	16.58%	20.44%	18.46%	9.21%
Highest fluctuation	0.15%	0.13%	0.18%	0.11%

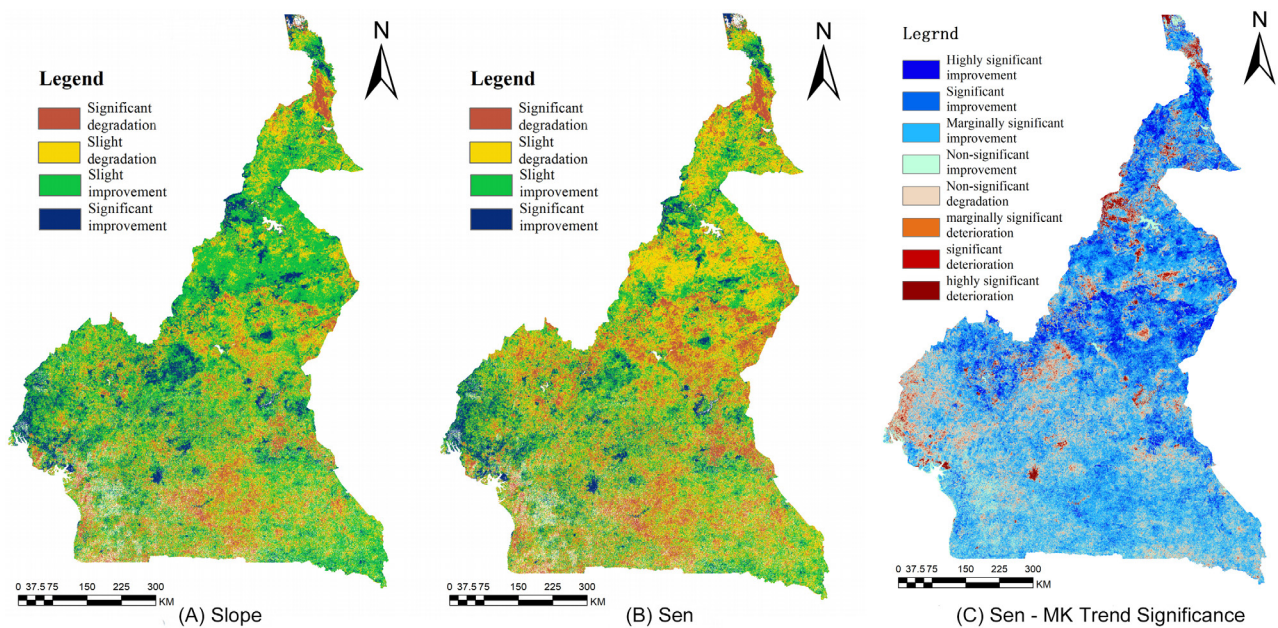


Fig. 6. Trend and significance analysis of fractional vegetation cover (FVC) in Cameroon using Slope, Theil-Sen, and Mann-Kendall Methods (2000-2022). a) Slope trend, b) Theil-Sen Median trend, and c) Sen-Mann-Kendall trend significance.

( $p < 0.05$ ) in 60% of areas. Additional Slope details and Sen & Mann-Kendall variants (Fig. S7) show consistent patterns, though with minor regional divergences. In areas where Slope and Sen diverge (15% pixels), discrepancies stem from topographic characteristics (steep slopes amplifying outliers), climatic variability (extreme events affecting non-median trends), and anthropogenic features (localized land-use causing non-linear shifts).

#### Climatic Factors

Precipitation shows a strong positive correlation with FVC in arid northern regions ( $r = 0.65$ , explaining 45% variance), promoting growth, while temperature exhibits negative effects in 33.5% of areas ( $r = -0.45$ , very significant in 14.42%), inhibiting vegetation under heat stress. Solar radiation has mixed impacts: non-significant positive correlations in 36.52% of regions, but inhibitory in southwestern areas due to increased

evaporation (Fig. S8 for temperature, precipitation, and solar radiation, and Fig. S9 for correlation stacked chart, highlighting north-south contrasts). These findings align with recent studies on soil erosion in steep forests and mangrove species distribution, emphasizing climatic-anthropogenic interactions.

In northern regions, land-use changes (e.g., agriculture, grazing, deforestation, quantified as 15% forest loss via ESA CCI) quantitatively compare with climatic drivers, explaining 55% of FVC decline variance vs. 35% from climatic factors (multiple regression:  $R^2 = 0.72$ ,  $p < 0.01$ ). The results highlight that anthropogenic drivers amplify climatic vulnerabilities, leading to greater FVC loss in affected areas.

#### Topographic Factors

Cameroon exhibits pronounced topographic differentiation, influencing vegetation distribution. Mid-low altitude regions (600-1000 m) reach peak FVC

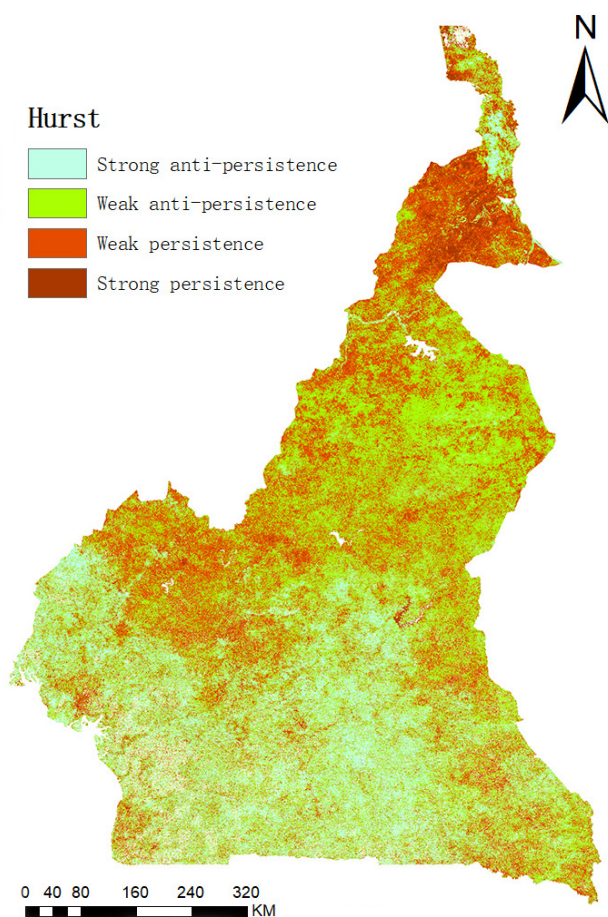


Fig. 7. Cameroon FVC persistence.

(0.75) in spring-summer months, while high-altitude areas (>1400 m) decline to 0.25 in autumn-winter due to severe climatic constraints like colder temperatures and reduced soil stability, inhibiting growth (Fig. S10 shows monthly FVC at different altitudes and pixel counts, with the majority in the 0-500 m range). Slope gradients of 0-10° support high FVC (0.75) in wet months, but >15° reduce it to 0.25 through erosion and instability (Fig. S10 for monthly FVC at slopes; Fig. S19 for pixel counts, dominated by 0-5°). Fig. S11 (topographic and slope characteristics) further illustrates these gradients, confirming topography's role in modulating FVC. Overall, topographic variables explain 40% of FVC variability nationwide (regression:  $R^2 = 0.40$ ).

### Hurst Analysis

Cameroon is home to rich biodiversity, yet its ecosystems face significant challenges, including deforestation, land degradation, and the impacts of climate change [37]. Understanding and predicting the potential for vegetation recovery is essential for developing effective ecological restoration and conservation strategies. These strategies play a crucial role in promoting sustainable development and ensuring the long-term protection of biodiversity

[38]. Fig. 7 illustrates significant spatial differentiation in vegetation cover persistence: the northern region exhibits predominantly weak anti-persistence, driven by urbanization, agricultural expansion, and climatic aridity, contributing to degradation; the central region shows mostly weak persistence, reflecting stable environments or effective protection measures; the southern region mixes anti-persistence and persistence, attributed to diverse ecosystems and land-use patterns, with primary forests stable and developed areas degraded.

Coverage statistics reveal that weak anti-persistence dominates (47.38%), strong anti-persistence accounts for 17.79%, weak persistence accounts for 31.45%, and strong persistence accounts for 3.38%. This highlights anti-persistence prevalence, indicating insufficient stability from human-climatic factors, with high weak anti-persistence underscoring degradation risks in northern and southern regions, requiring priority interventions [39].

### Limitations and Uncertainties

It is acknowledged that ground-based meteorological stations in Cameroon remain unevenly distributed and particularly sparse in the remote southern tropical rainforests and northern semi-arid zones. Although the CRU TS 4.06 gridded product integrates multiple reanalysis and station sources, residual spatial interpolation bias may still exist. Future work will incorporate denser in-situ networks and higher-resolution regional climate models to further reduce this uncertainty.

### Conclusions

This study presents a detailed analysis of the spatiotemporal variations in vegetation cover across Cameroon, focusing on the relationships between fractional vegetation cover (FVC), climate, and topographic factors from 2000 to 2022. By integrating MODIS EVI data, SRTM DEM, and CRU TS 4.06 climate data, the research provides new insights into how topography and climate interact to shape vegetation dynamics in different regions of Cameroon. The quantitative separation of drivers further demonstrates that anthropogenic pressures amplify climatic effects in vulnerable zones.

The findings reveal substantial regional variations in FVC, with the northern and southern regions facing significant ecological vulnerability due to climatic aridity, agricultural expansion, and human activities. The northern regions, in particular, experience low vegetation cover and high variability, exacerbated by desertification risks. Conversely, the central and southern regions benefit from more stable ecological conditions, with tropical rainforests and vegetation

cover supported by favorable climatic conditions, such as higher rainfall and milder temperatures.

The study underscores the complex interplay between climatic factors, such as precipitation, temperature, and solar radiation, and topographic factors, including elevation and slope. Precipitation plays a crucial role in promoting vegetation growth, especially in arid regions. However, the effects of temperature and solar radiation are more nuanced, with excessive heat and radiation acting as inhibitors of vegetation growth, particularly in the northern and southwestern regions.

A key finding of this study is the dominance of weak anti-persistence in vegetation cover across Cameroon, particularly in the northern and southern regions. This indicates insufficient stability in vegetation dynamics, driven by a combination of human and climatic factors. The analysis of vegetation recovery potential, using the Hurst exponent, further highlights the need for focused interventions in areas showing high degradation risks.

This research provides valuable insights for formulating effective ecological restoration and conservation strategies tailored to the specific challenges of each region. It calls for targeted actions in the northern and southern parts of Cameroon to mitigate vegetation degradation, enhance resilience to climate change, and promote sustainable land management practices. These findings contribute to the broader understanding of land-climate-ecosystem interactions in Central Africa, offering scientific guidance for climate adaptation and biodiversity conservation policies in the region.

### Acknowledgements

This research was funded by Hainan Province Science and Technology Special Fund of the Hainan Provincial Department of Science and Technology (ZDYF2022SHFZ323); the General Scientific Research Project of Zhejiang Provincial Department of Education (No. Y202455763); the out-of-university research project (No. HX2023F1013); Jiyang College of Zhejiang A&F University under Grant No. RQ1911F11. The authors express special thanks to the platforms Google Earth Engine (GEE) and the scholars who were engaged in relevant research.

### AI Usage Disclosure Statement

During the preparation of this work the authors used Doubao (ByteDance AI) and DeepSeek AI in order to assist in English language editing, grammatical correction and manuscript polishing. After using these tools, the authors reviewed and edited the content as needed and take full responsibility for the content of the published article.

### Author Contributions

Chuanxin Liu: Conceptualization, Methodology, Software, Investigation, Formal Analysis, Visualization, Writing–Original Draft (lead), Writing–Review & Editing (supporting).

Yong Du: Supervision, Funding Acquisition, Resources, Project Administration, Methodology/Validation (supporting), Writing–Review & Editing (lead).

Chunhua Shi: Resources, Validation, Writing–Review & Editing (supporting).

### Conflict of Interest

The authors declare no conflict of interest.

### References

1. ARIAS P.A., BELLOUIN N., COPPOLA E., JONES R.G., KRINNER G., MAROTZKE J., NAIK V., PALMER M.D., PLATTNER G.-K., ROGELJ J., ROJAS M., SILLMANN J., STORELVMO T., THORNE P.W., TREWIN B., ACHUTA RAO K., ADHIKARY B., ALLAN R.P., ARMOUR K., BALA G., BARIMALALA R., BERGER S., CANADELL J.G., CASSOU C., CHERCHI A., COLLINS W., COLLINS W.D., CONNORS S.L., CORTI S., CRUZ F.A., DENTENER F.J., DERECZYNSKI C., DI LUCA A., DIONGUE-NIANG A., DOBLAS-REYES F.J., DOSIO A., DOUVILLE H., ENGELBRECHT F., EYRING V., FISCHER E., FORSTER P., FOX-KEMPER B., FUGLESTVEDT J.S., FYFE J.C., GILLET N.P., GOLDFARB L., GORODETSKAYA I., GUTIÉRREZ J.M., HAMDI R., HAWKINS E., HEWITT H.T., HOPE P., ISLAM A.S., JONES C., KAUFMAN D.S., KOPP R.E., KOSAKA Y., KOSSIN J., KRAKOVSKA S., LEE J.-Y., LI J., MAURITSEN T., MAYCOCK T.K., MEINSHAUSEN M., MIN S.-K., MONTEIRO P.M.S., NGO-DUC T., OTTO F., PINTO I., PIRANI A., RAGHAVAN K., RANASINGHE R., RUANE A.C., RUIZ L., SALLÉE J.-B., SAMSET B.H., SATHYENDRANATH S., SENEVIRATNE S.I., SÖRENNSSON A.A., SZOPA S., TAKAYABU I., TREGUIER A.-M., VAN DEN HURK B., VAUTARD R., VON SCHUCKMANN K., ZAEHLE S., ZHANG X., ZICKFELD K. Technical summary. In: Masson-Delmotte V., Zhai P., Pirani A., Connors S.L., Péan C., Berger S., Caud N., Chen Y., Goldfarb L., Gomis M.I., Huang M., Leitzell K., Lonnoy E., Matthews J.B.R., Maycock T.K., Waterfield T., Yelekçi O., Yu R., Zhou B. (eds.) *Climate change 2021: the physical science basis*. Intergovernmental Panel on Climate Change, **2021**.
2. CHENG Y., HE G., LUO J., GU H. Effects of climate change on temperature sensitivity of vegetation growth in Huang-Huai-Hai Plain: Spatial-temporal dynamics and ecological adaptability. *Remote Sensing*, **16** (21), 4024, **2024**.
3. CHENG P., WU K., PAN Y. Spatiotemporal Variations of Fractional Vegetation Coverage and Its Driving Mechanisms in Southwestern China. *Forests*, **16** (5), 798, **2025**.
4. PIAO S., YUE C., DING J., GUO Z. Perspectives on the

- role of terrestrial ecosystems in the ‘carbon neutrality’ strategy. *Science China Earth Sciences*, **65**, 1178, **2022**.
5. YIN L., HUI Y. Estimation and spatiotemporal variation analysis of vegetation coverage on the Loess Plateau from 2000 to 2014 based on MODIS. *Environment and Sustainable Development*, **41** (3), 181, **2016** [In Chinese].
  6. DAN S. Spatiotemporal Responses of the Hulunbuir Grassland Ecosystem to Climate and Grazing Activities. Doctoral dissertation, Chinese Academy of Forestry, Beijing, China, **2020** [In Chinese].
  7. DENG MING Y., BAISA W., ZHILEI Y., JUNFENG W., YIN C. Spatiotemporal dynamics of land use pattern and analysis of vegetation coverage change in the Huaihe River Basin. *China Rural Water and Hydropower*, (11), 52, **2016** [In Chinese].
  8. MUJAWAMARIYA M., MANISHIMWE A., NTIRUGULIRWA B., ZIBERA E., GANSZKY D., NTAUWHIGANAYO BAHATI E., NYIRAMBANGUTSE B., NSABIMANA D., WALLIN G., UDDLING J. Climate Sensitivity of Tropical Trees Along an Elevation Gradient in Rwanda. *Forests*, **9** (10), 647, **2018**.
  9. WOODCOCK C.E., STRAHLER A.H. The factor of scale in remote sensing. *Remote Sensing of Environment*, **21** (3), 311, **1987**.
  10. LAN X., YIN Y., TANG J., LIAN Y., ZHAO F., WANG Y., ZHENG Z. Evaluation of surface latent heat and sensible heat fluxes from ERA-5, GLDAS, and MODIS on different underlying surfaces in the Tibetan Plateau. *Journal of Mountain Science*, **22** (1), 230, **2025**.
  11. LAI J., SHI Q. Coupled effects of climate change and human activities on vegetation dynamics in the Southwestern Alpine Canyon Region of China. *Journal of Mountain Science*, **21** (10), 3234, **2024**.
  12. DU Z., ZHANG X., XU X., ZHANG H., WU Z., PANG J. Quantifying influences of physiographic factors on temperate dryland vegetation, Northwest China. *Scientific Reports*, **7** (1), 40092, **2017**.
  13. TEUBNER I.E., FORKEL M., JUNG M., LIU Y.Y., MIRALLES D.G., PARINUSSA R., VAN DER SCHALIE R., VREUGDENHIL M., SCHWALM C.R., TRAMONTANA G., CAMPS-VALLS G., DORIGO W.A. Assessing the relationship between microwave vegetation optical depth and gross primary production. *International Journal of Applied Earth Observation and Geoinformation*, **65**, 79, **2018**.
  14. MADROÑERO PALACIOS S.M., MUÑOZ GUERRERO D.A. Projections of land-cover change in a tropical high-andean lake. *Civil Engineering Journal*, **11** (9), 3840, **2025**.
  15. THANH P.T., FREESHAN M., OSAMA N., CHIEN L.H., THOM T.T., ELSHEWY M.A. Soil Erosion Risk and Mitigation Strategies in Steep and Complex Forest Ecosystems. *Civil Engineering Journal*, **11** (8), 3358, **2025**.
  16. CASAL G., TRÉGAROT E., CORNET C.C., MCCARTHY T., GEEST M. A cost-effective method to map mangrove forest extent, composition, and condition in small islands based on Sentinel-2 data: Implications for management. *Ecological Indicators*, **159**, 111696, **2024**.
  17. BARATTO J., TERASSI P.M.D.B., GALVANI E. Changes in vegetation cover and the relationship with surface temperature in the Cananéia-Iguape Coastal System, São Paulo, Brazil. *Remote Sensing*, **16** (18), 3460, **2024**.
  18. WANG Q., LIANG L., WANG S., WANG S., ZHANG L., QIU S., SHI Y., SHI J., SUN C. Insights into spatiotemporal variations in the NPP of terrestrial vegetation in Africa from 1981 to 2018. *Remote Sensing*, **15** (11), 2748, **2023**.
  19. NLEND B., HUNEAU F., BOUM-NKOT S.N., SONG F., KOMBA D., GWODOG B., MEYOUPE P., DJIEUGOUE B., FONGO E. Review of isotope hydrology investigations on aquifers of Cameroon (Central Africa): What information for the sustainable management of groundwater resources. *Water*, **15** (23), 4056, **2023**.
  20. KANDJI S.T., VERCHOT L., MACKENSEN J. Climate change and variability in southern Africa: Impacts and adaptation in the agricultural sector. *Climatic Change*, **122** (3-4), 587, **2014**.
  21. MINEPDED. Annuaire Statistique du Ministère de L’Environnement et du Développement Durable. MINEPDED: Yaoundé, Cameroon, **2019** [In French].
  22. MOLUA E.L. Climatic trends in Cameroon: implications for agricultural management. *Climate Research*, **30** (3), 255, **2006**.
  23. GUENANG G.M., MKANKAM K.F. Onset, retreat and length of the rainy season over Cameroon. *Atmospheric Science Letters*, **13** (2), 255, **2012**.
  24. EBODÉ V.B. Analysis of the spatio-temporal rainfall variability in Cameroon over the period 1950 to 2019. *Atmosphere*, **13** (11), 1769, **2022**.
  25. VONDOU D.A., GUENANG G.M., DJIOTANG T.L.A., KAMSU-TAMO P.H. Trends and interannual variability of extreme rainfall indices over Cameroon. *Sustainability*, **13** (12), 6803, **2021**.
  26. MINISTRY OF COMMERCE, PRC. Country (Region) Guidelines for foreign investment and cooperation - Cameroon (2020 Edition); China Commerce Press: Beijing, China, **2020** [In Chinese].
  27. CARLSON T.N., RIPLEY D.A. On the relation between NDVI, fractional vegetation cover, and leaf area index. *Remote Sensing of Environment*, **62** (3), 241, **1997**.
  28. SU K., LIU H., WANG H. Spatial-temporal changes and driving force analysis of ecosystems in the Loess Plateau Ecological Screen. *Forests*, **13** (1), 54, **2022**.
  29. YU Y., LIU D., HU S., SHI X., TANG J. Spatiotemporal heterogeneity of vegetation cover dynamics and its drivers in coastal regions: evidence from a typical coastal province in China. *Remote Sensing*, **17** (5), 921, **2025**.
  30. XIA X., LIANG W., LV S., PAN Y., CHEN Q. Remote Sensing identification and stability change of alpine grasslands in Guoluo Tibetan Autonomous Prefecture, China. *Sustainability*, **16** (12), 5041, **2024**.
  31. SHI X., YANG D., ZHOU S., LI H., ZENG S., YIN C., YANG M. Analysis of Spatiotemporal variation characteristics and influencing factors of grassland vegetation coverage in the Qinghai-Tibet Plateau from 2000 to 2023 Based on MODIS Data. *Land*, **13** (12), 2127, **2024**.
  32. OLIVEIRA G.S., SOUZA J.P.S., CARDOZO É.P., PACHECO D.G., FERREIRA M.L., PICANÇO M.C., SOARES J.R.S., ALVES A.M.O.S., DE ANDRADE A.M., DA SILVA R.S. Correlation between the growth index and vegetation indices for irrigated soybeans using free orbital images. *AgriEngineering*, **7** (3), 67, **2025**.
  33. WANG X., HE W., HUANG Y., WU X., ZHANG X., ZHANG B. Exploring spatial non-stationarity and scale effects of natural and anthropogenic factors on net primary productivity of vegetation in the Yellow River Basin. *Remote Sensing*, **16** (17), 3156, **2024**.
  34. POTAPOV P., HANSEN M.C., LAESTADIOUS L., TURUBANOVA S., YAROSHENKO A., THIES C., SMITH W., ZHURAVLEVA I., KOMAROVA A., MINNEMEYER S., ESİPOVA E. The last frontiers of

- wilderness: tracking loss of intact forest landscapes from 2000 to 2013. *Science Advances*, **3**, e1600821, **2017**.
35. GUAN K., PAN M., LI H., WOLF A., WU J., MEDVIGY D., CAYLOR K.K., SHEFFIELD J., WOOD E.F., MALHI Y., LIANG M., KIMBALL J.S., SALESKA S.R., BERRY J., JOINER J., LYAPUSTIN A.I. Photosynthetic seasonality of global tropical forests constrained by hydroclimate. *Nature Geoscience*, **8**, 284, **2015**.
36. MILICH L., WEISS E. GAC NDVI interannual coefficient of variation (CoV) images: ground truth sampling of the Sahel along north-south transects. *International Journal of Remote Sensing*, **21** (2), 235, **2000**.
37. NKEMBI C., TCHOUTO T., DOUCET J.L. Land-cover change threatens tropical forests and biodiversity in the Littoral Region, Cameroon. *Oryx*, **55** (4), 687, **2021**.
38. CHEN Y., CHENG C., XIONG K., RONG L., ZHANG S. Quantifying the biodiversity and ecosystem service outcomes of karst ecological restoration: A meta-analysis of South China Karst. *Catena*, **245**, 108278, **2024**.
39. LIANG L., SUN Q., LUO X., WANG J.H., ZHANG L.P., DENG M.X., DI L.P., LIU Z.X. Long-term spatial and temporal variations of vegetative drought based on vegetation condition index in China. *Ecosphere*, **8** (8), e01919, **2017**.

## Supplementary Material

<https://www.pjoes.com/SuppFile/219363/1/>